IEEE Access
Multidisciplinary | Rapid Review | Open Access Journal

Received March 5, 2019, accepted March 19, 2019, date of publication March 21, 2019, date of current version April 3, 2019.

Digital Object Identifier 10.1109/ACCESS.2019.2906690

Centralized-Light-Source Two-Way PAM8/PAM4 FSO Communications With Parallel Optical Injection Locking Operation

WEN-SHING TSAI[1], HAI-HAN LU[2], (Senior Member, IEEE), CHUNG-WEI SU[2], ZHEN-HAN WANG[2], AND CHUNG-YI LI[3]

[1]Department of Electrical Engineering, Ming Chi University of Technology, New Taipei City 243, Taiwan
[2]Institute of Electro-Optical Engineering, National Taipei University of Technology, Taipei 106, Taiwan
[3]Department of Communication Engineering, National Taipei University, New Taipei City 237, Taiwan

Corresponding author: Hai-Han Lu (hhlu@ntut.edu.tw)

This work was supported by the Ministry of Science and Technology (MOST) of Taiwan under Grant 106-2221-E-131-018-MY2, Grant 107-2221-E-027-077-MY3, and Grant 107-2221-E-027-078-MY3.

ABSTRACT For the first time up to our knowledge, a centralized-light-source two-way eight-level pulse amplitude modulation (PAM8)/four-level pulse amplitude modulation (PAM4) free-space optical (FSO) communication with parallel optical injection-locked vertical-cavity surface-emitting laser (VCSEL) transmitter is practically demonstrated. With the assistance of parallel optical injection locking, injection locking in the polarization sideband causes a simultaneous generation of the free-running orthogonal polarization sideband to form a centralized-light-source scheme. With the centralized light source, additional light source or wavelength reuse component, such as Fabry–Perot laser diode or reflective semiconductor optical amplifier, is not needed at the receiver side. It is very attractive because it enables the receiver side to share the light source remotely located at the transmitter side. Based on the centralized-light-source scheme and parallel optical injection-locking operation, the injection-locked parallel polarization sideband is used for downlink transmission, and the induced free-running orthogonal polarization sideband is transmitted and used as the optical carrier for uplink transmission. Over a 200-m free-space link, good bit-error-rate (BER) performance, the qualified PAM8, and PAM4 eye diagrams are obtained for two-way FSO communications. This proposed centralized-light-source two-way FSO communication provides a practical choice for two-way high transmission capacities and considerably develops the scenario characterized by parallel optical injection locking.

INDEX TERMS Centralized-light-source, free-space optical communication, parallel optical injection locking, vertical-cavity surface-emitting laser.

I. INTRODUCTION

For a fixed bandwidth, eight-level pulse amplitude modulation (PAM8)/four-level pulse amplitude modulation (PAM4) enables three/two times the transmission rate compared with none-return-to-zero (NRZ). PAM8/PAM4 is thereby promisingly advantageous for providing high-transmission-rate [1]–[5]. Nevertheless, PAM8/PAM4 is more subject to noise than NRZ. It should give a higher price for a higher optical signal-to-noise ratio (OSNR) for optical PAM8/PAM4 signal transmission. Accordingly, PAM8/PAM4 is appropriate for building a high-speed but short-reach lightwave transmission. The polarization domain has been examined substantially for optical wireless communications. Parallel/orthogonally polarized dual-sideband operation is greatly matched with two-way free-space optical (FSO) communications [6]–[8]. Vertical-cavity surface-emitting laser (VCSEL) has excellent optical characteristics including low operation current, single longitudinal mode operation, and large modulation bandwidth. These characteristics make VCSEL useful for lightwave transmission systems. A single-mode VCSEL with parallel optical injection locking will excite a concurrent generation of the free-running orthogonal polarization sideband, indicating that injection-locked parallel polarization sideband and free-running orthogonal polarization

The associate editor coordinating the review of this manuscript and approving it for publication was Pallab K. Choudhury.

sideband occur at the same time [9]–[12]. Moreover, parallel optical injection locking exhibits a frequency response enhancement in parallel polarization. Parallel optical injection-locked VCSEL transmitter is thereby possessed a promising feature for affording a high-transmission-rate FSO communication.

For a practical deploying of two-way FSO communication, the receiver side requires an additional light source or a wavelength reuse component for upstream modulation. Fabry-Perot laser diode (FP LD) and reflective semiconductor optical amplifier (RSOA) are mostly employed in two-way FSO communications for upstream [13], [14]. For the FP LD, however, additional light source is needed for upstream carrier generation and transmission. As for the RSOA, nevertheless, RSOA with its limitation is not able to support high transmission capacity for upstream. In this study, a centralized-light-source two-way PAM8/PAM4 FSO communication that adopts a parallel optical injection-locked VCSEL transmitter is proposed and practically constructed. OSNRFor the first time up to our knowledge, this study is the pioneering one that adopts parallel optical injection locking operation in a centralized-light-source two-way PAM8/PAM4 FSO communication. Noticeably, injection-locked parallel polarization sideband and free-running orthogonal polarization sideband exist concurrently to form a centralized-light-source scheme. With a centralized-light-source scheme in the transmitter side for downlink and uplink transmissions, the receiver side is kept source-free [15], [16]. Such architecture is attractive because it enables the receiver side to share the light source remotely generated at the transmitter side. With centralized-light-source scheme and parallel optical injection locking operation, the injection-locked parallel polarization sideband is utilized as the downstream carrier for 84 Gb/s PAM8 signal modulation, and the induced free-running orthogonal polarization sideband is transmitted and utilized as the upstream carrier for 45 Gb/s PAM4 signal modulation. Mach-Zehnder modulator (MZM) is deployed at the receiver side to replace the traditional optical components of LD and RSOA for upstream modulation. The MZM provides a good platform to modulate 45 Gb/s PAM4 signal with one optical carrier (induced free-running orthogonal polarization sideband), which makes a breakthrough in upstream transmission capacity. A set of doublet lenses is adopted to operate a 200-m free-space transport in the 1550 nm wavelength [17], [18]. Through a 200-m free-space link, the link performance of the proposed centralized-light-source two-way PAM8/PAM4 FSO communication has been analyzed by bit error rate (BER) and eye diagrams. For downlink transmission, the link performance has been investigated in real-time for PAM8 eye diagrams and post-processing for BER values [19]. For uplink transmission, the link performance has been examined in real-time for PAM4 eye diagrams and BER values. BER measurement is executed by auto-searching using a one-channel error detector and the PAM4 3-eye (upper/middle/lower) sampling method [20]. With an in-depth investigation, competent BER performances, qualified PAM8 and PAM4 eye diagrams are attained at 84 Gb/s (downstream) and 45 Gb/s (upstream) operations through a 200-m free-space link.

System complexity and power dissipation are key concerns for the implementation of different modulation formats in FSO communications. For orthogonal frequency-division multiplexing (OFDM) modulation, the main problems of OFDM are its high peak to average power ratio and its sensitivity to phase noise and frequency offset. As for quadrature amplitude modulation (QAM) modulation, QAM modulation is more susceptible to the noise because QAM receiver is more complex compare to receivers of other modulation types. And further, as QAM utilizes amplitude component of signal to denote binary data, linearity needs to be maintained and thereby linear amplifier is required which spends more power. OFDM/QAM-OFDM FSO communications have been proposed in [21] and [22]. However, these OFDM/QAM-OFDM signals must be generated offline by MATLAB program and uploaded into an expensive arbitrary waveform generator (AWG). At the receiver side, these OFDM/QAM-OFDM signals must be calculated offline by MATLAB for the analysis of BER performance and the corresponding constellation map. In comparison with OFDM/QAM-OFDM FSO communications, PAM8/PAM4 FSO communication does not require expensive AWG (PAM8/PAM4) and complicated offline calculation (PAM4). Therefore, PAM8/PAM4 is preferable due to low power consumption and system simplicity. A previous study demonstrated a 12.5 Gb/s multi-channel broadcasting transmission for FSO communication based on the optical frequency comb module [23]. However, the free-space transmission rate of 12.5 Gb/s is far less than the corresponding value of 84 Gb/s (downstream) adopted in our proposed FSO communication. Moreover, a bidirectional fiber-invisible laser light communication and fiber-wireless convergence system with two orthogonally polarized optical sidebands was presented in [24]. Nevertheless, the free-space transmission rate of 10 Gb/s (downstream)/10 Gb/s (upstream) and the free-space link of 100 m are significantly less than the related values of 84 Gb/s (downstream)/45 Gb/s (upstream) and 200 m adopted in this proposed FSO communication. Additionally, a former research demonstrated a 9-Gbps/5-m QAM-OFDM visible light communication with a 450-nm GaN laser diode transmitter [22]. Nonetheless, the 9-Gbps/5-m are greatly less than the corresponding values of 84-Gb/s (downstream)/200-m adopted in such proposed FSO communication. This demonstrated centralized-light-source two-way PAM8/PAM4 FSO communication with a parallel optical injection-locked VCSEL transmitter is promising for the development of high-speed two-way optical wireless communications. It is superior to previous FSO communications [22]–[24] given its features for providing high transmission capacity with sufficient mobility.

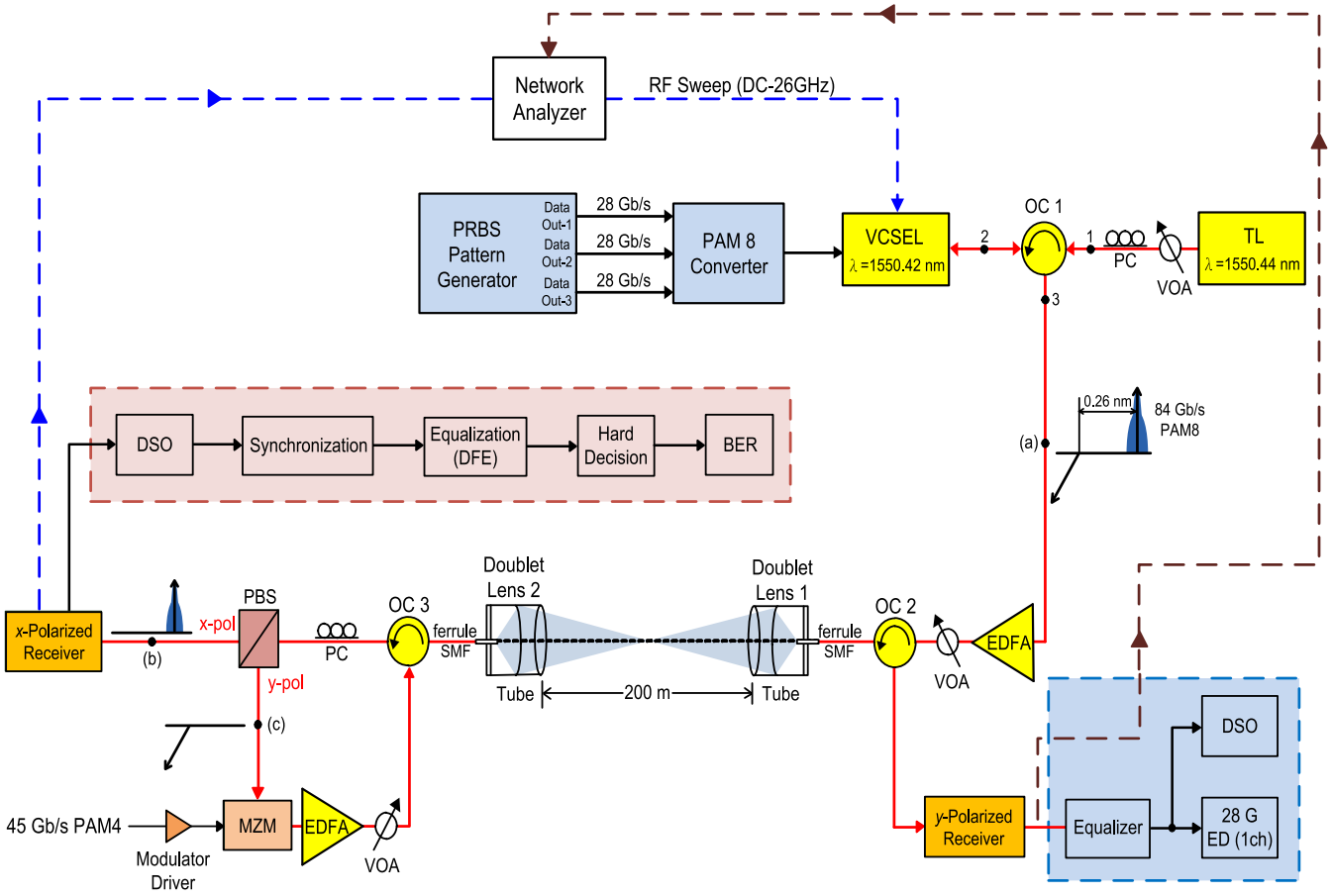

FIGURE 1. The framework of the offered two-way PAM8/PAM4 FSO communication with a parallel optical injection-locked VCSEL transmitter, and the measurement structure of the frequency response of two-way PAM8/PAM4 FSO communication.

II. EXPERIMENTAL SETUP

A. FRAMEWORK OF THE PROPOSED TWO-WAY PAM8/PAM4 FSO COMMUNICATIONS

The framework of the offered two-way PAM8/PAM4 FSO communications that adopts a parallel optical injection-locked VCSEL transmitter is presented in Fig. 1. Additionally, Table 1 summarizes the key physical parameters of the transmission setup. A three-channel pseudorandom binary sequence (PRBS) pattern generator generates three binary PRBS data streams at 28 Gb/s with a length of $2^{15}-1$. A PAM8 converter is used to transfer three 28 Gb/s NRZ signals into an 84 Gb/s PAM8 signal. After conversion, a VCSEL transmitter is directly modulated by an 84 Gb/s PAM8 signal. An optical carrier from the VCSEL is transmitted together with the PAM8 signal in the free-space channel to implement a direct amplitude modulated FSO communication. PAM8 linearity is an important parameter for PAM8 VCSEL-based FSO communication, a linear driver should be deployed after the PAM8 converter to enhance the PAM8 signal so as to operate the VCSEL in the linear region. Nevertheless, since that the power-driving current curve of VCSEL is very near the linear distribution, a linear driver to enhance the PAM8 signal is not required [25]. The light from a tunable laser (1550.44 nm) is injected into a VCSEL (1550.42 nm) via an integration of a variable optical attenuator (VOA), a polarization controller (PC), and an optical circulator (OC1). This single mode VCSEL, with a threshold current of 2 mA and a 3-dB bandwidth of 10.2 GHz, is aimed for high-speed and high-performance optical communications. The VOA is utilized to control the injected power level, and the PC is adjusted to ensure the behavior of parallel optical injection. The injection-locked parallel polarization (x-polarization) sideband with 84 Gb/s PAM8 signal and the induced free-running orthogonal polarization (y-polarization) sideband [insert (a)] are enhanced by an erbium-doped fiber amplifier (EDFA), attenuated by a VOA, and transmitted through a 200-m free-space link via two OCs (OC2 and OC3) and a set of doublet lenses. The output power and noise figure of EDFA are 17 dBm and 4.5 dB at an input power of 0 dBm, respectively. An atmospheric attenuation of approximately 1 dB exists for a 200-m free-space link. Thereafter, the light is split into two branches along the two orthogonally polarized sidebands using a PC with a polarization beam splitter. The PC is deployed to adjust the x-polarization [insert (b)] and y-polarization [insert (c)] sidebands. The x-polarization sideband with PAM8 signal is detected by an

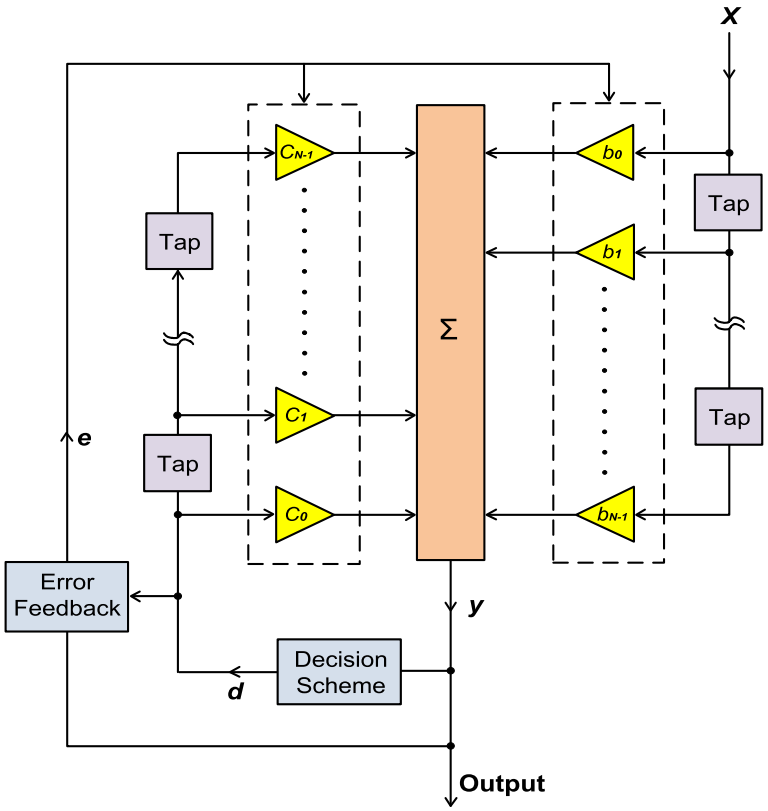

FIGURE 2. The functional diagram of the DFE.

x-polarized receiver with a 3-dB bandwidth of 25 GHz. The link performance of the proposed 84 Gb/s PAM8 FSO communication with a parallel optical injection-locked VCSEL transmitter is investigated in real-time for eye diagrams and post-processing for BER values. The PAM8 eye diagrams are caught using a digital storage oscilloscope (DSO), and the BER values are offline processed through the processes of synchronization, equalization, and hard decision. In the process of synchronization, a segment of 10k PAM8 symbols is windowed. After synchronization, a decision feedback equalizer (DFE) is adopted to compensate for the received PAM8 signal by removing the overall channel effects, including inter-symbol interference (ISI) and transceiver nonlinearity. Subsequently, a hard decision is adopted to recover the PAM8 signal.

For uplink transmission, the induced free-running orthogonal polarization (y-polarization) sideband is sent to a MZM which is modulated by a 45 Gb/s PAM4 signal. A two-channel PRBS pattern generator generates two binary PRBS data streams at 22.5 Gb/s with a length of $2^{15} - 1$. A PAM4 converter is used to transfer two 22.5 Gb/s NRZ signals into a 45 Gb/s PAM4 signal. The output of the MZM is boosted by an EDFA, controlled by a VOA, circulated by OC3, and sent to a 200-m free-space link. Afterwards, the upstream signal is circulated by OC2 and received by a y-polarized receiver with a 3-dB bandwidth of 20 GHz. After equalization by a linear equalizer, BER measurement is implemented by using a high-sensitivity one-channel error detector. In addition, a DSO is used to catch the PAM4 eye diagrams.

As to the frequency response, the measurement structure of the frequency response of two-way PAM8/PAM4 FSO communication is illustrated in Fig. 1 as well. RF sweep signal (DC – 26 GHz) generated from a network analyzer is supplied to the VCSEL. For x-polarization, after receiving by an x-polarized receiver, the RF sweep signal is sent back to the network analyzer. Whereas for y-polarization, after receiving by a y-polarized receiver, the RF sweep signal is sent back to the network analyzer. Thus, the frequency response of two-way PAM8/PAM4 FSO communication is measured for the states of free-running (x-polarization and y-polarization) and injection locking (x-polarization).

B. DECISION FEEDBACK EQUALIZER (DFE)

The functional diagram of the DFE is illustrated in Fig. 2. For DFE, x denotes the input,b_n denotes the feedforward coefficient, c_n denotes the feedback coefficient, y denotes the summation of weighted taps, d denotes the output of decision scheme, and e denotes the error from error feedback. The signal is sampled at an instant time of $t_0 + kT$ (t_0 is the initial time, T is the signal interval) to obtain the sum of the weighted taps y [26]:

$$y = \sum_{n=0}^{N-1} b_n x\,(t_0 + kT - nT) \tag{1}$$

TABLE 1. Key physical parameters of the transmission setup.

Parameter	Value
Modulation Format	PAM8 (84 Gb/s,downstream) PAM4 (45 Gb/s,upstream)
VCSEL • Bandwidth • Wavelength • Threshold Current	 10.2 GHz (free-running) 1550.42 nm 2 mA
FSO • Free-Space Link • Atmospheric Attenuation	 200 m 1 dB/200 m
EDFA • Power • Noise Figure	 17 dBm@input power = 0 dBm 4.5 dB
x-Polarized Receiver • Bandwidth	 25 GHz
y-Polarized Receiver • Bandwidth	 20 GHz

where n is an integer from 0 to N-1 ($n = 0, 1, 2, \ldots\ldots, N$-$1$). The error e is determined by the summation of weighted taps y and output decision d:

$$e = y - d \tag{2}$$

To estimate the channel effects, a sequence of training signal is placed in front of the data signal. Here, the output decision d is the training signal rather than received signal after decision. By utilizing the training signal, the channel response repeatedly updates the feedforward coefficient b_n and the feedback coefficient c_n:

$$b_n(k+1) = b_n(k) - u\,\mathrm{ex}\,(t_0 + kT - nT) \tag{3}$$

$$c_n(k+1) = c_n(k) + ued\,(t_0 + kT - nT) \tag{4}$$

where u is the step size. As running out the training signal, the coefficients b_n and c_n are stabilized, and d is then transferred to the received PAM8 signal. Since that the coefficients b_n and c_n are stabilized, the error e repeatedly updates the coefficients and thereby adaptively compensates for the received PAM8 signal as the output of the DFE. The hard decision after the DFE (Fig. 1) makes a decision based on the threshold level to recover the PAM8 signal. Both DFE and hard decision are contributed to obtaining good BER performance. They are very effective in reducing error propagation and improving BER performance.

III. EXPERIMENTAL RESULTS AND DISCUSSIONS

To have a close connection with parallel optical injection and induced free-running orthogonal polarization sideband, we adjust the parallel optical injection power level to observe the variation of the induced free-running orthogonal polarization sideband. Fig. 3(a), 3(b), and 3(c) presents the optical spectra of the VCSEL for the states of free-running [Fig. 3(a)], optimum parallel optical injection [Fig. 3(b)], and strong parallel optical injection [Fig. 3(c)]. The free-running VCSEL possesses a parallel polarization sideband at a wavelength of 1540.42 nm [Fig. 3(a)]. As the VCSEL is injection-locked (optimum parallel optical injection), the optical power of the parallel polarization sideband is enhanced and its optical spectrum is shifted to a slight longer wavelength at a wavelength of 1540.44 nm. Besides, injection locking in the polarization sideband induces a concurrent generation of the free-running orthogonal polarization sideband. Optimum parallel optical injection causes a larger amount of stimulated recombination of carriers [27], [28]. In this way, the orthogonal polarization sideband is induced and generated at its free-running frequency. The wavelength of free-running orthogonal polarization sideband is shorter than that of injection-locked parallel polarization sideband by 0.26 nm [Fig. 3(b)], signifying VCSEL with a birefringence of 32.5 GHz. However, it is to be observed that strong parallel optical injection causes a great power decrease corresponding to the orthogonal polarization sideband. The optical power of the orthogonal polarization sideband is approximately 37 dB lower than that of the parallel polarization sideband [Fig. 3(c)]. The optical power of parallel optical injection locking sideband (P_x) can be described by the injection power (P_{inj}) [9]–[12]:

$$P_x = \left(\frac{k}{2r}\right)^2 \frac{P_{\mathrm{inj}}}{1 + \left(\frac{\pi v_i}{r} + \alpha\right)^2} \tag{5}$$

where k denotes the field decay rate, r denotes the linear dichroism, v_i denotes the frequency detuning between the injection source and the parallel polarization sideband, and α denotes the linewidth enhancement factor. Clearly, from equation (5), P_x is proportional to P_{inj}. The optical power of parallel optical injection locking sideband increases with an increase in injection power. With parallel optical injection locking, the optical power of parallel polarization sideband will be enhanced. With optimum parallel optical injection, the optical power of induced free-running orthogonal polarization sideband (P_y) will be stimulated and generated. With strong parallel optical injection, the optical power of induced free-running orthogonal polarization sideband can be stated as [9]–[12]:

$$P_y = \frac{\mu}{1 - \frac{r}{k}} - 1 - P_x \tag{6}$$

where μ denotes the normalized bias current. Obviously, from equation (6), P_y decreases with an increase in P_x. With strong parallel optical injection, nevertheless, the optical power of induced free-running orthogonal polarization sideband decreases with an increase in the optical power of parallel optical injection locking sideband. With strong parallel optical injection, the optical power of induced orthogonal

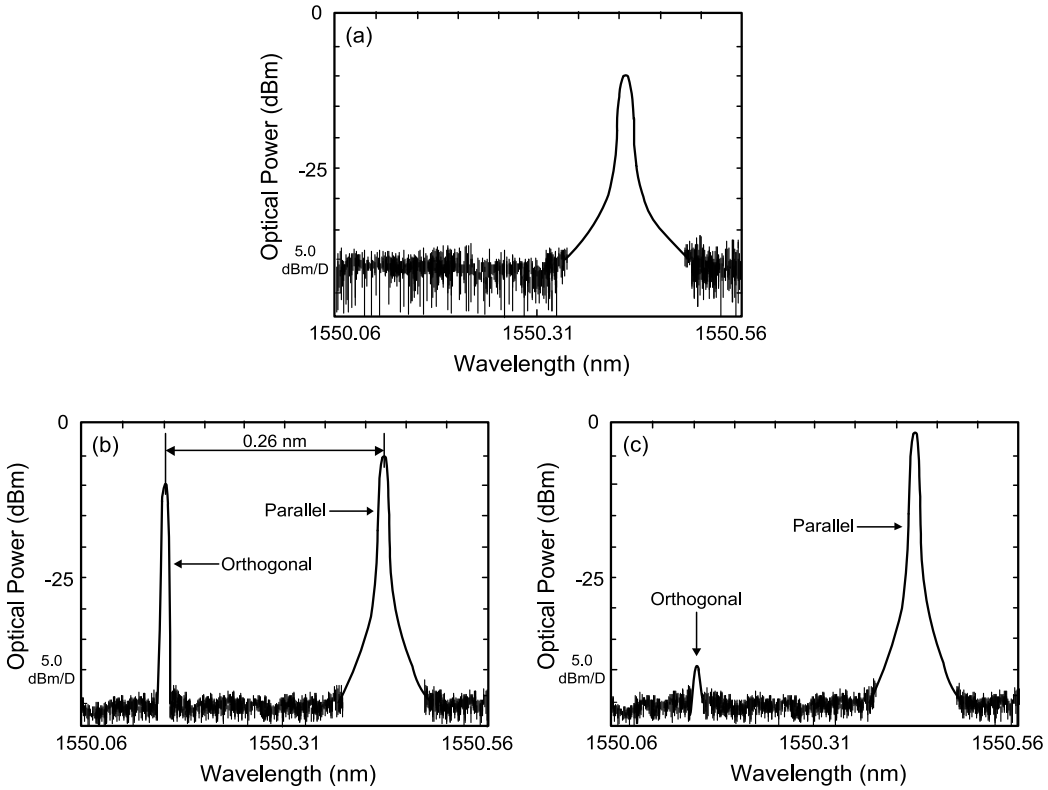

FIGURE 3. Optical spectra of the VCSEL for the states of (a) free-running, (b) optimum parallel optical injection, and (b) strong parallel optical injection.

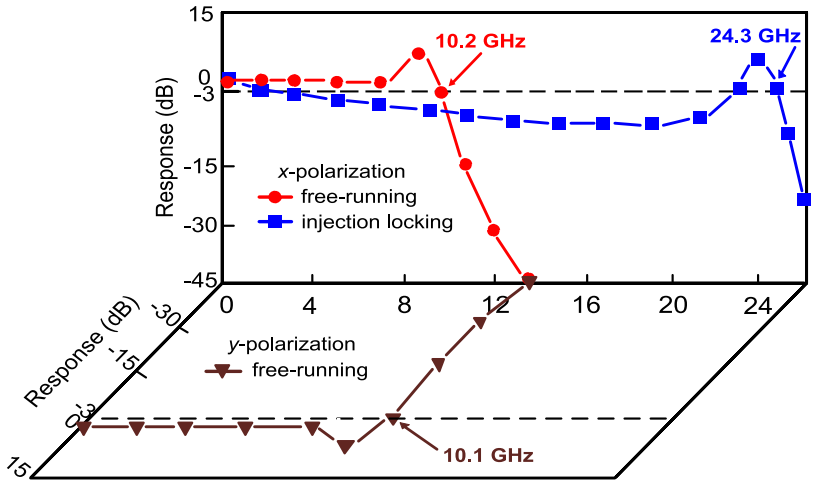

FIGURE 4. Frequency responses of two-way PAM8/PAM4 FSO communication under the scenarios of free-running (*x*-polarization and *y*-polarization) and injection locking (*x*-polarization).

polarization sideband will be considerably reduced at its free-running frequency.

The frequency responses of two-way PAM8/PAM4 FSO communication under the scenarios of free-running (*x*-polarization and *y*-polarization) and injection locking (*x*-polarization) are shown in Fig. 4. For *x*-polarization, clearly, the 3-dB bandwidth can be as high as 24.3 GHz. Optical injection locking is one of the most promising candidates to conquer the 3-dB bandwidth bottleneck. The 3-dB bandwidth can be greatly enhanced (1.0.2 GHz → 24.3 GHz) by utilizing optical injection locking technique. With parallel optical injection locking, an 84 Gb/s PAM8 FSO

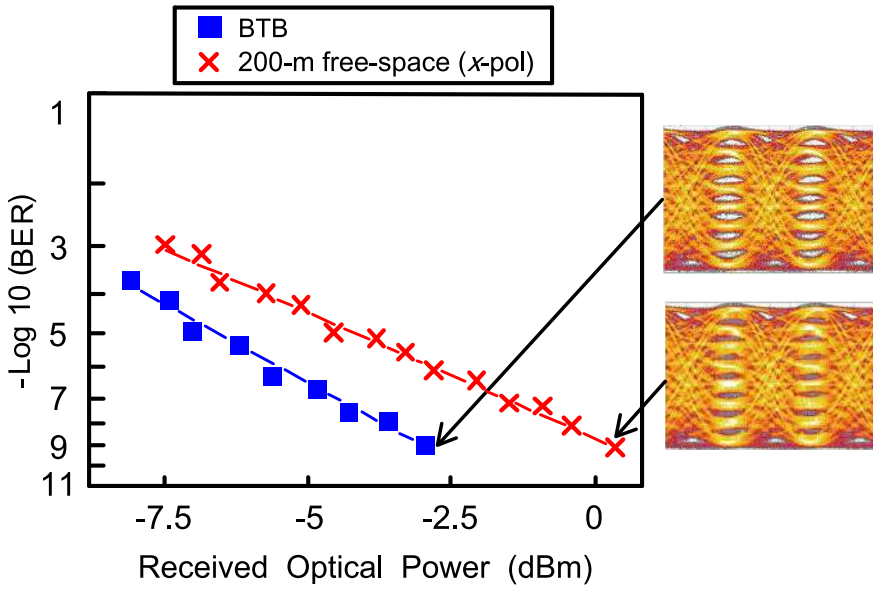

FIGURE 5. For downlink transmission, the BER performances of 84 Gb/s PAM8 signal for BTB state and through 200-m free-space transmission (*x*-polarization).

communication [$24.3\times\sqrt{2}\times3$ (PAM8 modulation) $>$ 84] can be satisfactorily developed for downlink transmission [29]. As for *y*-polarization, a 10.1-GHz 3-dB bandwidth is attained under the scenario of free-running. The figure shows the 3-dB bandwidths for free-running scenario (*x*- and *y*-polarizations) are closely the same, representing that the effect by polarization is almost none. Given that MZM with a 40-GHz 3-dB bandwidth, a 45 Gb/s PAM4 FSO communication can be satisfactorily built for uplink transmission.

For downlink transmission, the BER performances of 84 Gb/s PAM8 signal for back-to-back (BTB) state and through 200-m free-space transmission (*x*-polarization) are displayed in Fig. 5. At a BER value of 10^{-9}, a power penalty of 3.3 dB exists between the states of BTB and over 200-m free-space transmission. Good BER performance of 10^{-9} is chiefly resulted in the DFE process to remove the overall channel effects. Receiver with DFE is an effective approach to overcome the ISI and transceiver nonlinearity problems. The 3.3 dB power penalty is mainly ascribed to the atmospheric attenuation due to 200-m free-space transmission, coupling loss between the laser beam and the ferrule of optical fiber, and link loss due to noise from stray light received by the receiver. The atmospheric attenuation can be expressed by the exponential Beers-Lambert Law [30]–[36]:

$$\tau(z) = \frac{P(z)}{P_0} = e^{-\sigma z} \tag{7}$$

where $\tau(z)$ denotes the transmittance after transmitting z distance, z is the free-space transmission distance, P_0 is the laser power at the transmitter side, $P(z)$ is the laser power after transmitting z distance, and σ is the atmospheric attenuation coefficient. The exact value of the atmospheric attenuation coefficient σ varies with different weather types. In clear weather ($\sigma = 0.1$), through a 200-m (0.2-km) free-space link the atmospheric attenuation can be calculated as:

$$\tau(z) = \frac{P(z)}{P_0} = e^{-\sigma z} \tag{8}$$

In this work, a 200-m free-space transmission produces 1 dB atmospheric loss. This demonstrated 200-m free-space transmission satisfies the availability requirement of FSO communications. Over a 200-m free-space transmission, the atmospheric attenuation can change from 1 dB (clear weather) to 50 dB (bad weather) [35]. High atmospheric attenuation in bad weather results in the unavailability of FSO communications. Moreover, through a 200-m free-space link, it is vital to fit the laser beam size to the aperture area of fiber collimator to avoid large coupling loss and maintain the free-space link workably. Since that the laser beam is very narrow and the aperture area of fiber collimator is extremely small, operating the free-space transmission to work as if the optical fibers were linked is critical. If the laser beam size is smaller than the aperture area of fiber collimator (laser beam with a small divergence angle), then there is a small coupling loss at the receiver end. Thereby, better BER performance is obtained because of more optical power coupled into the optical fiber. By contrast, if the laser beam size is larger than the aperture area of fiber collimator (laser beam with a large divergence angle), then there is a large coupling loss at the receiver end. Thereby, worse BER performance is obtained because of less optical power coupled into the optical fiber. And further, since PAM8 is more subject to noise than PAM4, yet link loss due to noise from stray light received by the receiver affects the link budget. An atmospheric attenuation of around 1 dB exists for a 200-m free-space link, a coupling loss of around 1.5 dB exists between the laser beam and the ferrule of the optical fiber, and a link loss of around 0.7 dB exists due to noise from stray

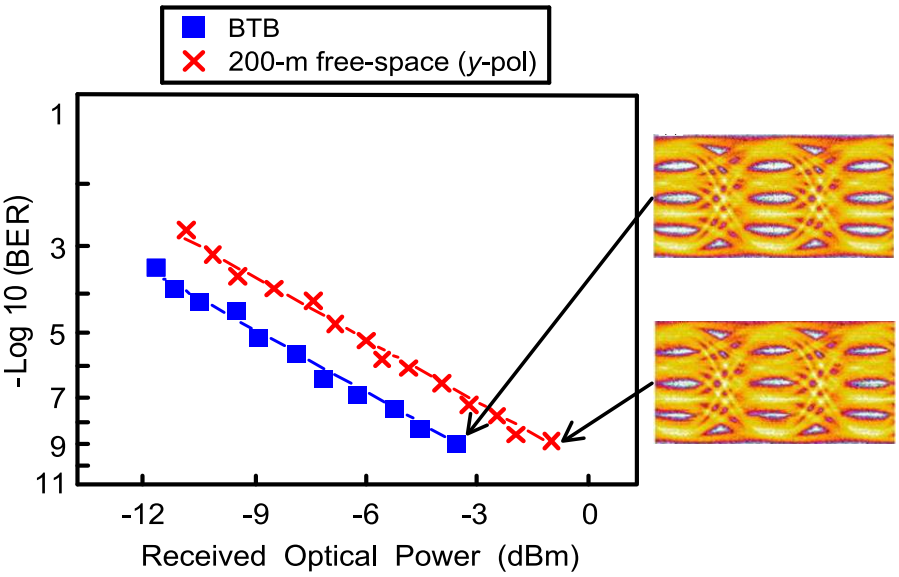

FIGURE 6. For uplink transmission, the BER values of 45 Gb/s PAM4 signal for BTB for the scenario and over 200-m free-space transmission (*y*-polarization).

light received by the receiver. Thus, a link budget of 3.2 dB (1 + 1.5 + 0.7) exists. The link budget of 3.2 dB is close to the power penalty of 3.3 dB. The eye diagrams of the 84 Gb/s PAM8 signal over 200-m free-space transmission are displayed in Fig. 5 as well. It can be seen that clear PAM8 eye diagrams exist for BTB state. Additionally, PAM8 eye diagrams with acceptable quality exist for the state of over 200-m free-space transmission. For BTB state, the received optical power is −2.8 dBm to obtain a 10^{-9} BER operation. For the state of over 200-m free-space transmission, the received optical power is 0.5 dBm to compensate for the OSNR reduction and to obtain a 10^{-9} BER operation. The OSNR for the state of over 200-m free-space transmission satisfies the minimum requirement of 10^{-9} BER operation. Thereby, the eye opening for BTB is bigger than that for 200-m free-space transmission.

For uplink transmission, the BER performances of 45 Gb/s PAM4 signal for BTB scenario and over 200-m free-space transmission (*y*-polarization) are presented in Fig. 6. At a BER value of 10^{-9}, a low power penalty of 2.5 dB exists between the scenarios of BTB and over 200-m free-space transmission. A low power penalty of 2.5 dB is primarily attributed to atmospheric attenuation due to 200-m free-space transmission and coupling loss between the laser beam and the ferrule of the optical fiber. Given that PAM8 is more susceptible to the noise than PAM4, the power penalty between the scenarios of BTB and over 200-m free-space transmission for PAM4 is lower than that for PAM8. An atmospheric attenuation of about 1 dB exists for a 200-m free-space link, and a coupling loss of about 1.5 dB exists between the laser beam and the ferrule of the optical fiber. Thus, a link budget of 2.5 dB (1 + 1.5) exists. The link budget of 2.5 dB matches the power penalty of 2.5 dB. As for eye diagrams, the eye diagrams of the 64 Gb/s PAM4 signal over 200-m free-space transmission are also displayed in Fig. 6. It can be found that clear PAM4 eye diagrams exist for BTB scenario. In addition, PAM4 eye diagrams with good characteristic exist for the scenario of over 200-m free-space transmission. This finding reveals that, with parallel optical injection locking at the transmitter side, a 1550-nm VCSEL transmitter with induced free-running orthogonal polarization sideband is adequately effective for a 45 Gb/s PAM4 uplink transmission.

For the future extension of two-way FSO communications, multi-channel transmission in each direction can be deployed to set up an ultra-high-speed two-way PAM8/PAM4 FSO communication. The free-space transmission rate can be considerably increased by dense-wavelength-division-multiplexing (DWDM) and space-division-multiplexing (SDM) schemes. DWDM scheme, which utilizes different optical wavelengths to transport the integrated data signals, is anticipated to improve the overall transmission rate of two-way FSO communications. SDM scheme, which multiplexes and de-multiplexes optical channels in the free-space, is anticipated to provide ultrahigh transmission rate in two-way FSO communications. A DWDM/SDM two-way PAM8/PAM4 FSO communication will afford the benefits of optical wireless communications for ultrahigh transmission capacity with sufficient flexibility.

IV. SUMMARY AND CONCLUSION

A centralized-light-source two-way PAM8/PAM4 FSO communication over 200-m free-space transmission is demonstrated for the first time. With parallel optical injection locking, injection-locked parallel polarization sideband and induced free-running orthogonal polarization sideband exist simultaneously so as to realize a centralized-light-source scheme. With centralized-light-source, the receiver side can be kept source-free. It is attractive because additional light

source or wavelength reuse component is not required at the receiver side. Injection-locked parallel polarization sideband is used as the downstream carrier for 84 Gb/s PAM8 signal transmission, and induced free-running orthogonal polarization sideband is delivered and utilized as the upstream carrier for 45 Gb/s PAM4 signal transmission. Brilliant BER performance, qualified PAM8 and PAM4 eye diagrams are attained for downstream and upstream modulations. Such demonstrated centralized-light-source PAM8/PAM4 FSO communication is shown to be a promising solution for affording high-transmission-rate and opening a door to speed up wide applications in two-way FSO communications.

REFERENCES

[1] Y. Fu, M. Bi, D. Feng, X. Miao, H. He, and W. Hu, "Spectral efficiency improved 2D-PAM8 trellis coded modulation for short reach optical system," *IEEE Photon. J.*, vol. 9, no. 4, Aug. 2017, Art. no. 7904908.

[2] D. Che, F. Yuan, and W. Shieh, "Towards high-order modulation using complex modulation of semiconductor lasers," *Opt. Express*, vol. 24, no. 6, pp. 6644–6649, Mar. 2016.

[3] G. W. Lu *et al.*, "Flexible generation of 28 Gbps PAM4 60 GHz/80 GHz radio over fiber signal by injection locking of direct multilevel modulated laser to spacing-tunable two-tone light," *Opt. Express*, vol. 26, no. 16, pp. 20603–20613, Aug. 2018.

[4] H.-H. Lu *et al.*, "45??Gb/s PAM4 transmission based on VCSEL with light injection and optoelectronic feedback techniques," *Opt. Lett.*, vol. 41, no. 21, pp. 5023–5026, Nov. 2016.

[5] R. Motaghiannezam *et al.*, "52 Gbps PAM4 receiver sensitivity study for 400GBase-LR8 system using directly modulated laser," *Opt. Express*, vol. 24, no. 7, pp. 7374–7380, Apr. 2016.

[6] C. Y. Li *et al.*, "Real-time PAM4 fiber-IVLLC and fiber-wireless hybrid system with a parallel/orthogonally polarized dual-wavelength scheme," *OSA Continuum*, vol. 1, no. 2, pp. 320–331, Oct. 2018.

[7] B. Wu *et al.*, "Polarization-insensitive remote access unit for radio-over-fiber mobile fronthaul system by reusing polarization orthogonal light waves," *IEEE Photon. J.*, vol. 8, no. 1, Feb. 2016, Art. no. 7200108.

[8] H.-Y. Wang, Y.-C. Chi, and G.-R. Lin, "Remote beating of parallel or orthogonally polarized dual-wavelength optical carriers for 5G millimeter-wave radio-over-fiber link," *Opt. Express*, vol. 24, no. 16, pp. 17654–17669, Aug. 2016.

[9] F. D. L. Coarer *et al.*, "Polarization dynamics induced by parallel optical injection in a single-mode VCSEL," *Opt. Lett.*, vol. 42, no. 11, pp. 2130–2133, Jun. 2017.

[10] H. Lin, S. Ourari, T. Huang, A. Jha, A. Briggs, and N. Bigagli, "Photonic microwave generation in multimode VCSELs subject to orthogonal optical injection," *J. Opt. Soc. Amer. B*, vol. 34, no. 11, pp. 2381–2389, Nov. 2017.

[11] A. Quirce *et al.*, "Polarization switching and injection locking in vertical-cavity surface-emitting lasers subject to parallel optical injection," *Opt. Lett.*, vol. 41, no. 11, pp. 2664–2667, Jun. 2016.

[12] A. Hurtado, A. Quirce, A. Valle, L. Pesquera, and M. J. Adams, "Nonlinear dynamics induced by parallel and orthogonal optical injection in 1550 nm vertical-cavity surface-emitting lasers (VCSELs)," *Opt. Express*, vol. 18, no. 9, pp. 9423–9428, Apr. 2010.

[13] H. H. Lu *et al.*, "Bidirectional fiber-wireless and fiber-VLLC transmission system based on an OEO-based BLS and a RSOA," *Opt. Lett.*, vol. 41, no. 3, pp. 476–479, Feb. 2016.

[14] M. Zhu *et al.*, "An upstream multi-wavelength shared PON based on tunable self-seeding fabry-Pérot laser diode for upstream capacity upgrade and wavelength multiplexing," *Opt. Express*, vol. 19, no. 9, pp. 8000–8010, Apr. 2011.

[15] H. H. Lu *et al.*, "Two-way lightwave transmission system with a centralized-light-source and VCSEL-based upstream wavelength selector," *OSA Continuum*, vol. 1, no. 4, pp. 1195–1204, Dec. 2018.

[16] F. Grassi, J. Mora, B. Ortega, and J. Capmany, "Centralized light-source optical access network based on polarization multiplexing," *Opt. Express*, vol. 18, no. 5, pp. 4240–4245, Feb. 2010.

[17] X.-H. Huang *et al.*, "WDM free-space optical communication system of high-speed hybrid signals," *IEEE Photon. J.*, vol. 10, no. 6, Dec. 2018, Art. no. 7204207.

[18] C.-Y. Li *et al.*, "A high-speed and long-reach pam4 optical wireless communication system," *IEEE Photon. J.*, vol. 10, no. 4, Aug. 2018, Art. no. 7906109.

[19] Y. Wang, J. Yu, N. Chi, and G.-K. Chang, "Experimental demonstration of 120-Gb/s Nyquist PAM8-SCFDE for short-reach optical communication," *IEEE Photon. J.*, vol. 7, no. 4, Aug. 2015, Art. no. 7201805.

[20] K. Szczerba *et al.*, "30 Gbps 4-PAM transmission over 200 m of MMF using an 850 nm VCSEL," *Opt. Express*, vol. 19, no. 26, pp. B203–B208, Dec. 2011.

[21] C. L. Ying, H.-H. Lu, C.-Y. Li, C.-J. Cheng, P.-C. Peng, and W.-J. Ho, "20-Gbps optical LiFi transport system," *Opt. Lett.*, vol. 40, no. 14, pp. 3276–3279, Jul. 2015.

[22] Y.-C. Chi, D.-H. Hsieh, C.-T. Tsai, H.-Y. Chen, H.-C. Kuo, and G.-R. Lin, "450-nm GaN laser diode enables high-speed visible light communication with 9-Gbps QAM-OFDM," *Opt. Express*, vol. 23, no. 10, pp. 13051–13059, May 2015.

[23] J. Tan, Z. Zhao, Y. Wang, Z. Zhang, J. Liu, and N. Zhu, "12.5 Gb/s multichannel broadcasting transmission for free-space optical communication based on the optical frequency comb module," *Opt. Express*, vol. 26, no. 2, pp. 2099–2106, Jan. 2018.

[24] H. H. Lu *et al.*, "Bidirectional fiber-IVLLC and fiber-wireless convergence system with two orthogonally polarized optical sidebands," *Opt. Express*, vol. 25, no. 9, pp. 9743–9754, May 2017.

[25] Y.-C. Wang *et al.*, "A high-speed 84 Gb/s VSB-PAM8 VCSEL transmitter-based fiber-IVLLC integration," *IEEE Photon. J.*, vol. 10, no. 5, Oct. 2018, Art. no. 7203608.

[26] S. U. H. Qureshi, "Adaptive equalization," *Proc. IEEE*, vol. 73, no. 9, pp. 1349–1387, Sep. 1985.

[27] C.-H. Chang, L. Chrostowski, C. J. Chang-Hasnain, and W. W. Chow, "Study of long-wavelength VCSEL-VCSEL injection locking for 2.5-Gb/s transmission," *IEEE Photon. Technol. Lett.*, vol. 14, no. 11, pp. 1635–1637, Nov. 2002.

[28] P. Saboureau, J.-P. Foing, and P. Schanne, "Injection-locked semiconductor lasers with delayed optoelectronic feedback," *IEEE J. Quantum Electron.*, vol. 33, no. 9, pp. 1582–1591, Sep. 1997.

[29] C.-Y. Li, H.-H. Lu, X.-H. Huang, Y.-C. Wang, J.-C. Chang, and P.-H. Chew, "52 m /9 Gb/s PAM4 plastic optical fiber-underwater wireless laser transmission convergence with a laser beam reducer," *Chineses Opt. Lett.*, vol. 16, no. 5, May 2018, Art. no. 050101.

[30] H. K. Al-Musawi *et al.*, "Adaptation of mode filtering technique in 4G-LTE hybrid RoMMF-FSO for last-mile access network," *J. Lightw. Technol.*, vol. 35, no. 17, pp. 3758–3764, Sep. 1, 2017.

[31] A. E. Morra, K. Ahmed, and S. Hranilovic, "Impact of fiber nonlinearity on 5G backhauling via mixed FSO/fiber network," *IEEE Access*, vol. 5, pp. 19942–19950, 2017.

[32] M. A. Khalighi and M. Uysal, "Survey on free space optical communication: A communication theory perspective," *IEEE Commun. Surveys Tuts.*, vol. 16, no. 4, pp. 2231–2258, 4th. Quart., 2014.

[33] Y. Ren *et al.*, "Atmospheric turbulence effects on the performance of a free space optical link employing orbital angular momentum multiplexing," *Opt. Lett.*, vol. 38, no. 20, pp. 4062–4065, Oct. 2013.

[34] S. Bloom, E. Korevaar, J. Schuster, and H. Willebrand, "Understanding the performance of free-space optics," *J. Opt. Netw.*, vol. 2, no. 6, pp. 178–200, Jun. 2003.

[35] I. I. Kim, B. McArthur, and E. J. Korevaar, "Comparison of laser beam propagation at 785 nm and 1550 nm in fog and haze for optical wireless communications," *Proc. SPIE*, vol. 4214, pp. 26–37, Feb. 2001.

[36] H. Weichel, *Laser Beam Propagation in the Atmosphere*, Bellingham, WA, USA: SPIE, 1990.

WEN-SHING TSAI received the M.S. and Ph.D. degrees from the Department of Electro-Optical Engineering, National Taipei University of Technology (NTUT), Taiwan, in 2003 and 2006, respectively. Since 2006, he has been an Assistant Professor with the Department of Electrical Engineering, Ming Chi University of Technology, where he was promoted to an Associate Professor, in 2012. His research interests include free-space optical (FSO) communications, fiber-wireless convergent systems, and eight-level pulse amplitude modulation (PAM8)/four-level pulse amplitude modulation (PAM4) transmission systems.

HAI-HAN LU (SM'08) received the M.S. and Ph.D. degrees from the Institute of Electro-Optical Engineering, National Central University, Taiwan, in 1991 and 2000, respectively.

Since 2003, he has been an Associate Professor with the Department of Electro-Optical Engineering, National Taipei University of Technology (NTUT), where he was promoted to a Professor, a Distinguished Professor, and a Lifetime Distinguished Professor, in 2003, 2006, and 2017, respectively. He has authored or co-authored more than 200 papers in SCI cited international journals and more than 130 papers in international conferences. His research interests include free-space optical (FSO) communications, UWOC transport systems, FSO-UWOC convergence, fiber-FSO convergence, and four-level pulse amplitude modulation (PAM4)/eight-level pulse amplitude modulation (PAM8) transmission systems. He is currently a Senior Member of OSA and a Fellow of SPIE and IET. He was a recipient of the Sun Yat-Sen Academic Award (Natural Science), in 2017, the National Invention Award (Gold Medal), in 2016, the ICT Month Innovative Elite Products Award, in 2014 and 2016, the Outstanding Electrical Engineering Professor Award from the Chinese Institute of Engineering, in 2015, the Outstanding Engineering Professor Award from the Chinese Engineer Association, in 2013, and the Outstanding Research Award from NTUT, in 2004, for his significant technical contributions to FSO communications, UWOC, PAM4/PAM8 transmission systems, fiber-FSO convergence, and fiber-wireless convergence.

CHUNG-WEI SU was born in Taipei, Taiwan, in 1995. He received the bachelor's degree from Tamkang University, New Taipei City, Taiwan, in 2017. He is currently pursuing the M.S. degree with the Institute of Electro-Optical Engineering, National Taipei University of Technology (NTUT), Taiwan. His research interests include free-space optical (FSO) communications and fiber-FSO convergence.

ZHEN-HAN WANG was born in Kaohsiung, Taiwan, in 1995. He received the B.S. degree from National Formosa University, Yunlin County, Taiwan, in 2017. He is currently pursuing the M.S. degree with the Institute of Electro-Optical Engineering, National Taipei University of Technology (NTUT), Taiwan. His research interests include fiber-free-space optical (FSO) and fiber-wireless convergent systems.

CHUNG-YI LI received the M.S. and Ph.D. degrees from the Department of Electro-Optical Engineering, National Taipei University of Technology (NTUT), Taiwan, in 2008 and 2012, respectively. From 2013 to 2014, he was an Engineer with the Innovation and Product Development Department, FOCI Fiber Optic Communications, Inc., Hsinchu, Taiwan. Since 2014, he has been a Research Assistant Professor with the Department of Electro-Optical Engineering, NTUT. Since 2018, he has been an Assistant Professor with the Department of Communication Engineering, National Taipei University (NTU). His research interests include free-space optical (FSO) communications, UWOC, and fiber-FSO convergence.